Abdominal Radiology

Published online: 6 June 2016

Abdom Radiol (2016) 41:1411–1430
DOI: 10.1007/s00261-016-0735-6

The gamut of primary retroperitoneal masses: multimodality evaluation with pathologic correlation

Guillermo P. Sangster,[1] Matias Migliaro,[2] Maureen G. Heldmann,[3] Peeyush Bhargava,[3] Alireza Hamidian,[4] Jaiyeola Thomas-Ogunniyi[5]

[1]Departments of Radiology and Anesthesiology, LSU Health – Shreveport, 1501 Kings Highway, Shreveport, LA 71103, USA
[2]Hospital Santa Isabel de Hungria, Mendoza 5521, Argentina
[3]Department of Radiology, LSU Health – Shreveport, 1501 Kings Highway, Shreveport, LA 71103, USA
[4]Department of Surgery, LSU Health – Shreveport, 1501 Kings Highway, Shreveport, LA 71103, USA
[5]Department of Pathology, LSU Health – Shreveport, 1501 Kings Highway, Shreveport, LA 71103, USA

Abstract

The retroperitoneum is a large space where primary and metastatic tumors grow silently before clinical signs appear. Neoplastic retroperitoneal diseases may be solid or cystic, primary or secondary and range from benign to aggressive in behavior. Retroperitoneal neoplasms are notable for their widely disparate histologies. The solid primary retroperitoneal neoplasms are extremely uncommon and can be classified based on their tissue of origin into three main categories: mesodermal tumors, neurogenic tumors, and extragonadal germ cell tumors. These tumors can grow to a large size before clinical symptoms occur or become palpable. When symptoms do occur, they are nonspecific. The majority of these masses are malignant and imaging plays a pivotal role in the detection, staging, and pre-operative planning. Benign and malignant masses should be distinguished whenever possible to avoid unnecessary surgical procedures. Macroscopic fat, calcification, necrosis, vascularity, and neural foraminal widening are common imaging features helping for tumor differentiation. Meticulous cross-sectional imaging can triage the patient to the most appropriate therapy. Tumor morphology dictates imaging character, and biologic activity is reflected by positron emission tomography (PET). Complete surgical excision with tumor free margins is essential for long-term survival. Biopsy should be performed in consultation with surgical oncology to avoid complicating curative surgery. This pictorial essay illustrates the spectrum of multidetector computed tomography (MDCT) imaging findings in common and uncommon primary retroperitoneal masses, with an emphasis on cross-sectional imaging features for an adequate tumor characterization and staging.

Key words: Retroperitoneum—Primary—Sarcomas—Tumors—Masses

Primary retroperitoneal neoplasms are rare, accounting for 0.1% to 0.2% of all malignancies [1], and approximately 70% to 80% are malignant [2]. Tumors can arise from any retroperitoneal tissue outside of the major retroperitoneal organs, and neoplasms can be divided primarily into solid and cystic masses. The solid neoplasms can be classified based on their tissue of origin into three main categories: mesodermal tumors, neurogenic tumors, and extragonadal germ cell tumors [2]. The preferred treatment of retroperitoneal sarcomas (RS) is surgical resection. However, complete excision is only possible in 20% to 75% of cases due to invasion of vital organs or vascular structures. Even with complete excision, recurrence rates are high for all subtypes of sarcoma [1]. Metastasis is common in high-grade sarcomas and spread occurs hematogenously to the liver, lung, bone, and brain [1].

CME activity This article has been selected as the CME activity for the current month. Please visit https://ce.mayo.edu/content/abdominal-radiology-journal-gamut-primary-retroperitoneal-masses%C2%A0-multimodality-evaluation and follow the instructions to complete this CME activity.

Electronic supplementary material The online version of this article (doi:10.1007/s00261-016-0735-6) contains supplementary material, which is available to authorized users.

Correspondence to: Guillermo P. Sangster; *email:* gsangs@lsuhsc.edu

Table 1. TNM classification

TNM	
T (primary site)	
T1	Tumor size ≤ 5 cm
T2	Tumor size > 5 cm
a	Superficial tumor
b	Deep tumor
N (lymph node involvement)	
Nx	Inability to evaluate the regional lymph nodes
N0	Absence of lymph nodes involvement
N1	Histologically verified regional lymph node metastasis
M (distant metastasis)	
M0	Absence of distant metastasis
M1	Presence of distant metastasis
G (histologic grade of malignancy)	
G1	Low, well differentiated
G2	Intermediate, moderately well differentiated
G3	Poorly or very poorly differentiated

Table 2. Tumor staging: American Joint Committee staging of soft-tissue sarcomas

Stage	Classification
IA	G1, T1, N0, M0
IB	G1, T2, N0, M0
IIA	G2, T1, N0, M0
IIB	G2, T2, N0, M0
IIIA	G3, T1, N0, M0
IIIB	G3, T2, N0, M0
IIIC	G1–3, T1, 2, N1, M0
IVA	G1–3, T3, N0, N1, M0
IVB	G1–3, T1–3, N0, N1, M1

The American Joint Committee Staging System of extremity soft-tissue sarcomas, which is based on the TNM classification, is commonly used for the staging of the retroperitoneal sarcomas [3]. The stage is determined by the size of the tumor, the histologic grade, spread to lymph nodes, and distant metastasis. We will briefly review the principles of the TNM classification used for sarcoma staging in Tables 1 and 2.

Mesodermal tumors

Mesodermal tumors constitute 47% to 57% of the primary retroperitoneal tumors (Table 3) [1], the vast majority of which (90%) are sarcomas [4]. Yet only 10% to 20% of all sarcomas arise from the retroperitoneum, with an overall incidence of 0.3% to 0.4% per 100,000 of the general population [3]. RS occur in all ages groups, with a peak in the fifth decade of life. RS tend to enlarge in retroperitoneal spaces without producing symptoms and are therefore often large at the time of diagnosis and present later with nonspecific symptoms such as abdominal pain and fullness. Liposarcomas, leiomyosarcomas, and malignant fibrous histiocytomas (MFH) constitute more than 80% of these tumors [2]. Recently, the frequency of MFH in the retroperitoneum has been disputed. With the use of immunohistochemistry, many of these fibrous tumors have now been shown to represent other sarcoma types such as leiomyosarcomas or dedifferentiated liposarcomas. For this reason, it is expected that the number of the reported MFH will be significantly reduced in the future [3].

Liposarcoma

Liposarcoma is the most common (33%) primary RS [2]. Liposarcoma can be sub-classified into three groups: well-differentiated liposarcoma with and without dedifferentiated components, myxoid and round-cell liposarcoma, and pleomorphic liposarcoma [5]. These subtypes have radiologic, clinical, pathologic, and genetic distinctions;

Table 3. Mesodermal tumors: characteristic imaging findings and other diagnosis features

Mesodermal tumors	Image finding	Other diagnosis features
Well-differentiated liposarcoma	Pure fat-containing mass Enhancing nodular septa	FDG-PET/TC image shows in the majority of low-grade liposarcomas faint or weak FOG uptake
Dedifferentiated liposarcoma	Heterogeneous mass with fat 30% calcifications	The nonadipose solid component of dedifferentiated liposarcoma is well demarcated Intense FOG uptake
Myxoid liposarcoma	Cystic appearance lesions with delayed progressive enhancement	Myxoid stroma Variable FOG uptake, although often weak
Pleomorphic liposarcoma	Nonspecific Heterogeneous soft-tissue mass with areas of necrosis	Do not contain fat on imaging FOG uptake
Leiomyosarcoma	Large mass, with extensive necrosis, contiguous involvement of a vessel	Calcifications are uncommon
Malignant fibrous histiocytoma	Nonspecific Heterogeneously enhancing soft-tissue mass with areas of necrosis and hemorrhage. 7% to 20% calcifications	Calcification and less extensive necrosis are tools to distinguish from leiomyosarcoma
Rhabdomyosarcoma	Nonspecific Mass lesion with areas of calcification, necrosis, and heterogeneous enhancement	Bimodal distribution, with peaks in occurrence at 7 years and at adolescence
E-GIST	Well-defined inhomogeneous mass with peripheral calcification	Positive marker CD117 (KIT protein)
Lipoma	Pure fat-containing mass without enhancement or soft tissue component	Difficult to distinguish from well-differentiated liposarcoma component
Leiomyoma	Similar to leiomyosarcoma	Almost exclusively in women

however, they can coexist in the same patient (histologically mixed subtypes) (Fig. 1). The well-differentiated forms are low-grade malignancies, which usually contain an appreciable amount of fat and rarely metastasize. However, the myxoid liposarcoma with round-cell components and the pleomorphic types show more aggressive behavior, may have a lesser amount of adipose tissue and appear similar to other sarcomas, and generally show higher rates of metastases [6–8].

Unfortunately, surgery is only curative in a minority of patients, and liposarcoma shows a high rate of local recurrence even when surgical margins are negative for tumor [8]. Liposarcoma frequently recurs within several years, most frequently within 6 months to 2 years, after the initial surgical resection. In routine follow-up computed tomography (CT) examinations, recurrent tumors were found to occur not only along the resection site but also anywhere else in the abdominal cavity [7, 8]. CT examinations are useful for the diagnosis and post-operative follow-up of patients with liposarcoma. Recurrent liposarcomas can be difficult to differentiate from normal retroperitoneal fat on imaging. In cases where CT evaluation shows soft-tissue attenuation at the site of a previous resection, a recurrence may not be easily distinguished from post-operative scarring or fibrosis in the surgical bed [3]. One suggested follow-up scheme is to obtain imaging at regular intervals (i.e., CT or magnetic resonance imaging (MRI) every 3–4 months for 2 years, then every 4–6 months for 3–5 years, and every 12 months thereafter). Follow-up for greater than 5 years is recommended. Although most sarcomas (including high-grade) recur within 2 years, marked delay in appearance of recurrent disease is not unusual [3].

The *well-differentiated* (Fig. 2) subtype is the most common type of retroperitoneal liposarcoma. It contains mature fatty tissue with imaging characteristics that may be indistinguishable from those of a benign lipoma. Furthermore, lipoma is less common than liposarcoma in the retroperitoneum. Well-differentiated retroperitoneal liposarcomas often recur if a clear margin is not obtained during surgical excision; however, they do not metastasize [4]. On imaging, liposarcomas demonstrate the CT attenuation and MRI signal intensity characteristics of fat. They are usually lobulated, displacing, or surrounding normal structures. Unlike lipomas, liposarcoma has thicker, irregular, and nodular septa that show enhancement after contrast material administration. They also may contain solid-appearing regions that are poorly defined, with no clear demarcation between the tumor and the surrounding fat. These areas usually enhance after administration of contrast material. In a majority of low-grade liposarcomas, the 18F-fluorodeoxyglucose positron emission tomography (FDG-PET/TC) imaging shows faint or weak FDG uptake [9].

Dedifferentiated liposarcoma (also called well-differentiated liposarcoma with dedifferentiated component) represents a subgroup of well-differentiated liposarcoma, where a portion of the tumor histologically differentiates into a nonadipose cell type such as fibrous tissue,

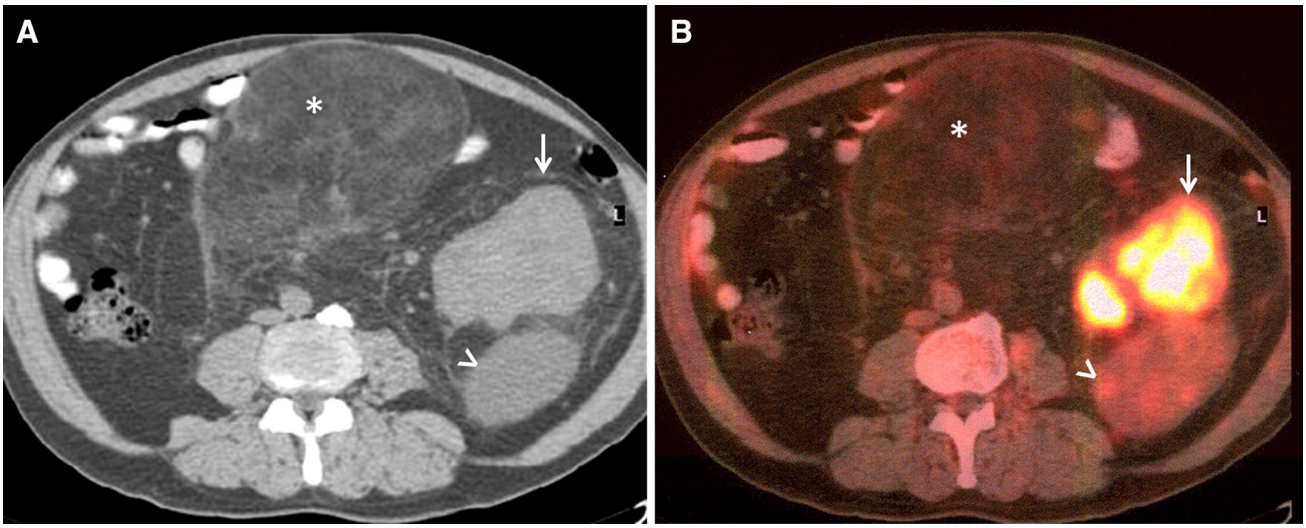

Fig. 1. Three synchronous retroperitoneal liposarcomas in a single patient. **A** Axial contrast-enhanced computed tomography (CT) of the abdomen. **B** Axial 18F-fluorodeoxyglucose positron emission tomography (FDG-PET)/CT image. Extensive ill-defined fat-containing mass (*asterisk*) causing anterior displacement of the small bowel loops. Minimal FDG activity is seen on the PET/CT fusion image. Histology confirmed a well-differentiated liposarcoma. A second soft-tissue lesion with intense metabolic activity and lack of perceptible fat is identified in the left perinephric space consistent with dedifferentiated liposarcoma (*arrow*). The posterior left renal fossa lesion (*arrowhead*) appears slightly hypodense compared with muscle density. On FDG-PET/CT fusion image, the lesion demonstrates a moderate metabolic activity. The final diagnosis was myxoid liposarcoma.

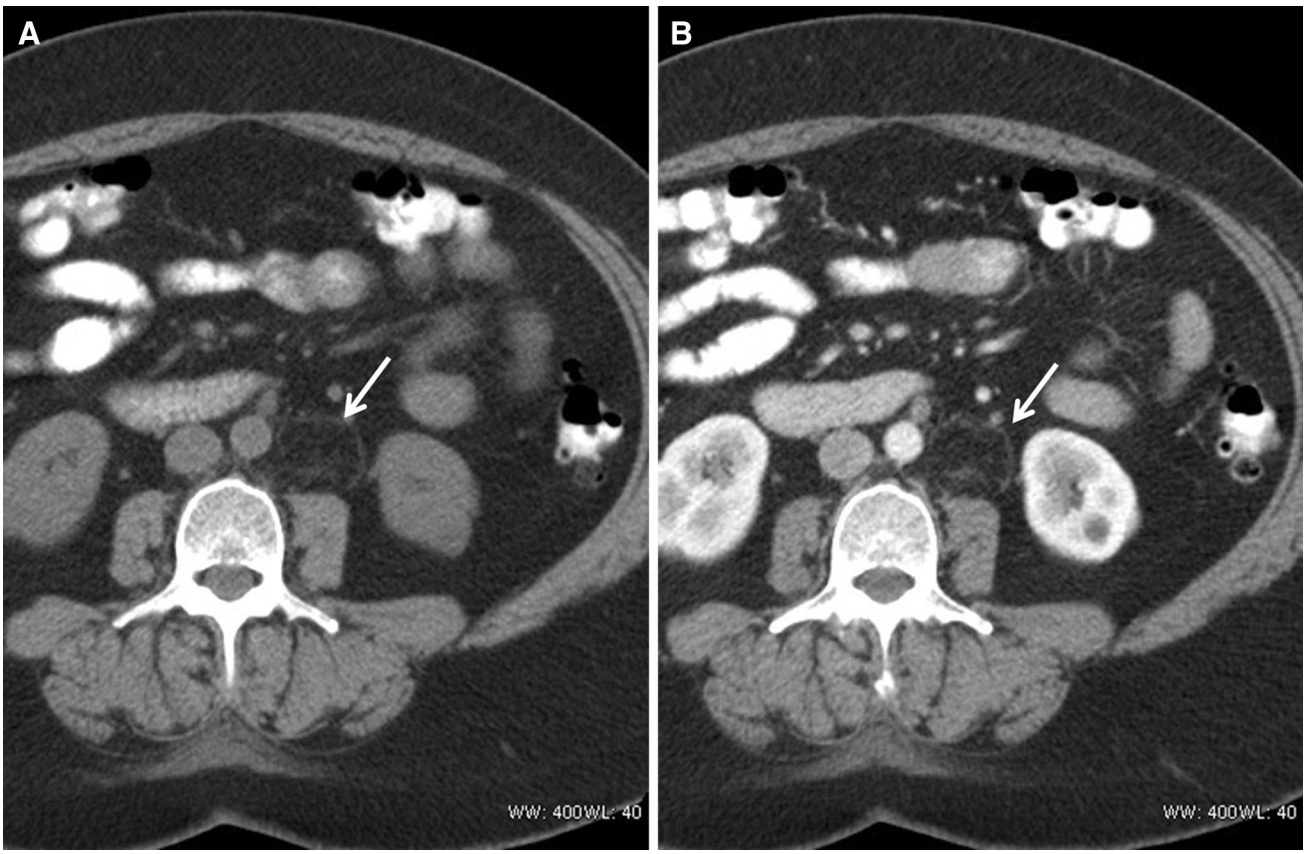

Fig. 2. Well-differentiated retroperitoneal liposarcoma. Axial noncontrast (**A**) and contrast-enhanced (**B**) CT abdomen shows a poorly delineated nonenhancing fat-containing mass with minimal interspersed soft-tissue components occupying the left latero-aortic space (*arrows*).

histiocyte, striated muscle, or contractile fiber cell [4]. Seventy-five percent of all dedifferentiated liposarcomas occur in the retroperitoneum; however, the progression to dedifferentiation is thought to depend on time rather than location [5]. This dedifferentiation represents progression of a tumor that has only the potential for local recurrence to one with full malignant potential, with a 17% chance of metastasis [4]. On imaging, the nonadipose solid component of dedifferentiated liposarcoma is well demarcated with distinct planes between the fat and the solid components. CT attenuation, MRI signal characteristics, and enhancement pattern of dedifferentiated liposarcomas are nonspecific, regardless of the cell types. Calcifications within a liposarcoma are seen in as many as 30% of cases and have proved to be a sign of poor prognosis, often indicating dedifferentiation [2]. On FDG-PET/CT images, there is a moderate FDG uptake component in the solid portion of theses tumors [9].

Myxoid liposarcomas occur in a slightly younger patient population and typically within the extremities, especially the deep muscles of the thigh and buttocks. Myxoid liposarcoma is occasionally found in the retroperitoneum [5]. These tumors contain myxoid fatty components and nonadipose tissue. Due to high-water content, these tumors are described as "cystic appearance lesions" on images. On noncontrast CT imaging, the attenuation is lower than that of adjacent muscle tissues, but they are not iso-attenuated relative to pure fluid. On MRI imaging, these tumors also have low-signal intensity on T1-weighted images and high-signal intensity on T2-weighted images. The intraluminal fat content of the tumor can appear as lacy, linear, or amorphous areas of high-signal intensity on T1-weighted images and intermediate signal on T2-weighted images. Myxoid liposarcoma demonstrates slowly progressive, reticular enhancement with contrast administration, which differentiates this lesion from a simple cyst [4]. On FDG-PET/CT images, myxoid liposarcomas demonstrate weak FDG uptake [7, 9].

Pleomorphic liposarcomas are aggressive tumors that commonly metastasize [4]. They are heterogeneous soft-tissue masses with areas of necrosis but no recognizable amount of fat on imaging, and indistinguishable from other solid tumors. Pleomorphic liposarcomas usually present with an increased FDG uptake on the FDG-PET/CT images [7, 9].

Leiomyosarcomas

Leiomyosarcomas are the second most frequent primary retroperitoneal tumor (28%) and are most commonly observed in women between the fifth and sixth decades [2, 4]. They arise from the smooth muscle tissue within the retroperitoneum, walls of retroperitoneal veins, or from embryonic Wolffian remnants [7]. These tumors can grow to a large size before compromising adjacent organs and precipitating clinical symptoms such as venous thrombosis [2]. Approximately, 40% of patients have metastases to liver, lungs, or lymph nodes at the time of diagnosis, which occur late in the course of the disease [2, 4]. Three major growth patterns have been identified: 62% are completely extravascular and extraluminal (Fig. 3), 33% are extravascular and intravascular (Figs. 4, 5), and only 5% are completely intravascular and intraluminal (Fig. 6) [4, 7]. These tumors can be larger than 10 cm and may contain extensive areas of necrosis with occasional hemorrhage. Calcifications are uncommon. [2]. The diagnosis of leiomyosarcoma should be suspected when there is a large retroperitoneal mass with necrosis and contiguous involvement of a vessel [2]. At CT, small tumors may be homogeneously solid, but large tumors are heterogeneous due to intralesional necrosis and hemorrhage. At MRI imaging, these tumors have intermediate- to low-signal intensity on T1-weighted images and intermediate- to high-signal intensity on T2-weighted images, depending on the amount of necrosis. Contrast enhancement is often heterogeneous and predominantly peripheral. Rarely, leiomyosarcoma may appear as mostly cystic.

Fig. 3. Extravascular leiomyosarcoma. Axial contrast-enhanced CT abdomen demonstrates a well-defined lobulated soft-tissue mass in the anterior pararenal space (*arrow*). This lesion produces compression and displacement of the pancreatic tail.

Malignant fibrous histiocytoma (MFH)

MFH is the third most common primary retroperitoneal tumor (19%) and overall the most common soft-tissue sarcoma in the body [2, 7]. After the extremities, the retroperitoneal space is the second most common site for this tumor (15% of these tumors occur in the retroperitoneum). MFH arises from undifferentiated mesenchymal cells, and it is more common in males in their fifth and sixth decades of life. Retroperitoneal MFHs are difficult to diagnose preoperatively because CT and MRI imaging appearances are nonspecific. Images demonstrate a large, infiltrating, and heterogeneously enhancing soft-tissue mass with areas of necrosis and hemorrhage and with invasion of adjacent organs [2]. Contrast enhancement is typically heterogeneous, and

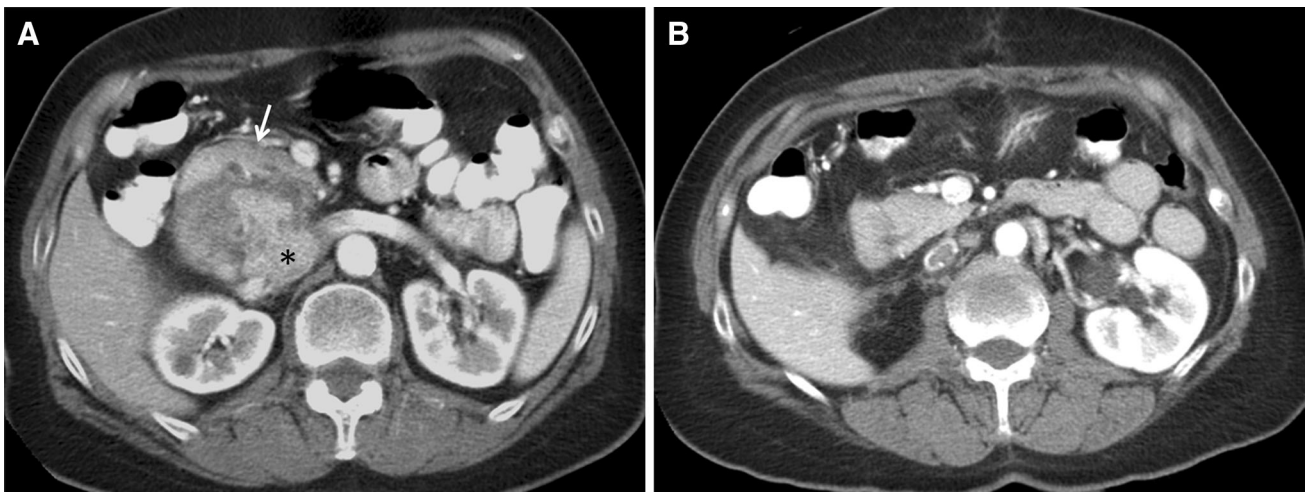

Fig. 4. Leiomyosarcoma with extravascular and intravascular growth. **A** Axial contrast-enhanced CT abdomen shows a well-defined lobulated enhancing mass (*arrow*) arising from the inferior vena cava (IVC) (*asterisk*). Intralesional heterogeneity is secondary to tumor necrosis and hemorrhage. **B** Postsurgical contrast CT of the abdomen demonstrates complete tumoral excision with IVC graft placement (*arrowhead*).

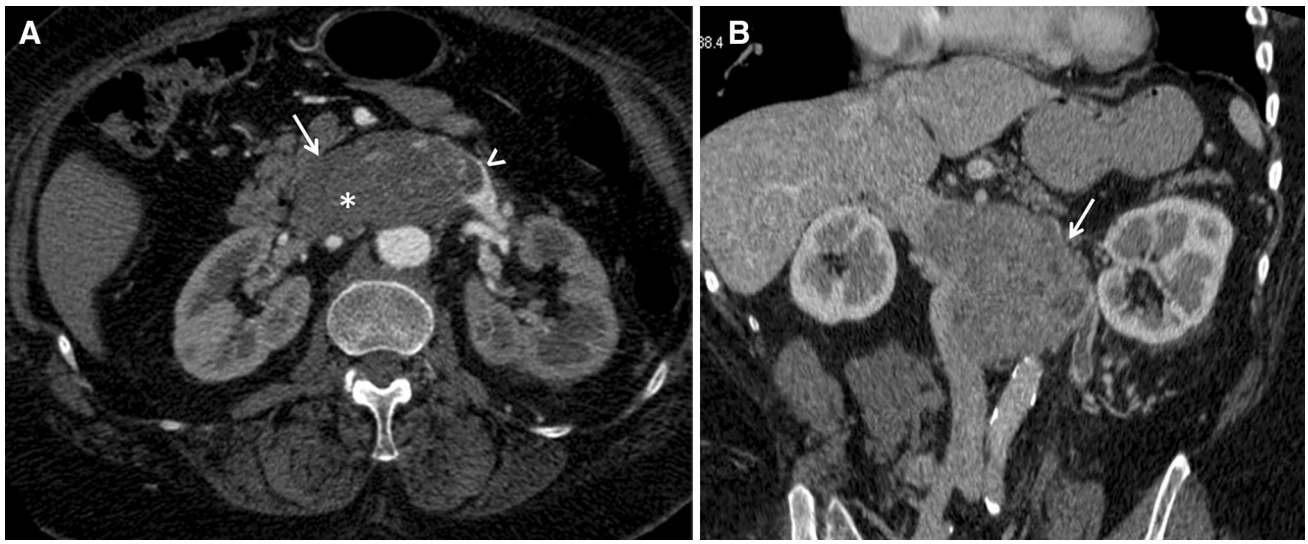

Fig. 5. Leiomyosarcoma with extravascular and intravascular patterns. Axial (**A**) and coronal (**B**) contrast-enhanced CT abdomen shows a well-defined heterogeneously enhancing retroperitoneal mass (*arrow*), with involvement of the left renal vein (*arrowhead*) and the IVC (*asterisk*). The expansion of the vascular lumen and enhancing component distinguish tumor thrombus from bland clot.

calcifications may be seen in 20% of cases [4]. The presence of calcification (Fig. 7) and less extensive areas of necrosis are tools that may help to distinguish MFH from leiomyosarcoma.

Rhabdomyosarcoma

Rhabdomyosarcoma is a malignant tumor with striated muscle origin. Rhabdomyosarcoma has a bimodal distribution in the pediatric population, with peaks of occurrence at 7 years and during adolescence. The retroperitoneum is involved in 7% of cases [2]. Rhabdomyosarcoma is divided into five major histologic categories: embryonal, alveolar, botryoid embryonal, spindle cell embryonal, and anaplastic. Unfortunately, the appearance of the mass itself is nonspecific and indistinguishable from other sarcomas. CT or MRI imaging shows a mass lesion with areas of calcification, necrosis, and heterogeneous enhancement (Fig. 8). The location and demographics of the patient are most useful in narrowing the differential. Metastases occur in 10% to 20% of cases.

Extra-gastrointestinal stromal tumor

Gastrointestinal stromal tumors (GIST) represent less than 1% of all malignancies, but they are the most common mesenchymal neoplasms in the gastrointestinal tract (40% to 70% originate from the stomach, 20% to 40% from small intestine, 5% to 15% from the colon and rectum, and 5% from the esophagus) [10]. GIST arises from the wall of the gastrointestinal tract and is thought to originate from the interstitial cells of Cajal. The most specific and important immunohistochemical marker is the KIT (CD117) protein, a tyrosine kinase growth factor receptor expressed in more than 95% of cases. More rarely, neoplasms with histology and immunohistochemistry similar to GISTs may occur outside the gastrointestinal tract (omentum, mesentery, and retroperitoneum) and are so-called extra-gastrointestinal stromal tumors (EGISTs) [10]. EGISTs arising in the retroperitoneum are extremely rare.

On imaging, small GISTs usually appear as well-defined homogeneous masses; large tumors tend to be ill-defined and heterogeneous, sometimes with calcification and necrosis (Fig. 9). Malignant GISTs are typically large and well defined, with a heterogeneous rim of soft tissue with lower signal intensity than that of the contrast material-enhanced liver. Central fluid attenuation is seen in 67% of cases [11]. EGISTs from the retroperitoneum are uncommon so radiological findings have not been well described. Takao et al. described a case in which CT and MRI showed a large, well-defined heterogeneous mass with peripheral calcification in the retroperitoneum [11]. These findings are similar to those described for the large GIST of the GI tract, except for peripheral calcification. These tumors are difficult to distinguish from those of other sarcomas that may arise in the retroperitoneum. PET/CT imaging with F-18FDG has evolved as the standard of care for the staging of gastrointestinal stromal tumors (GISTs). Most GIST tumors are FDG avid and show intense FDG uptake on pretreatment scan and is also a useful modality for monitoring response to treatment, specifically with targeted molecular drugs [9].

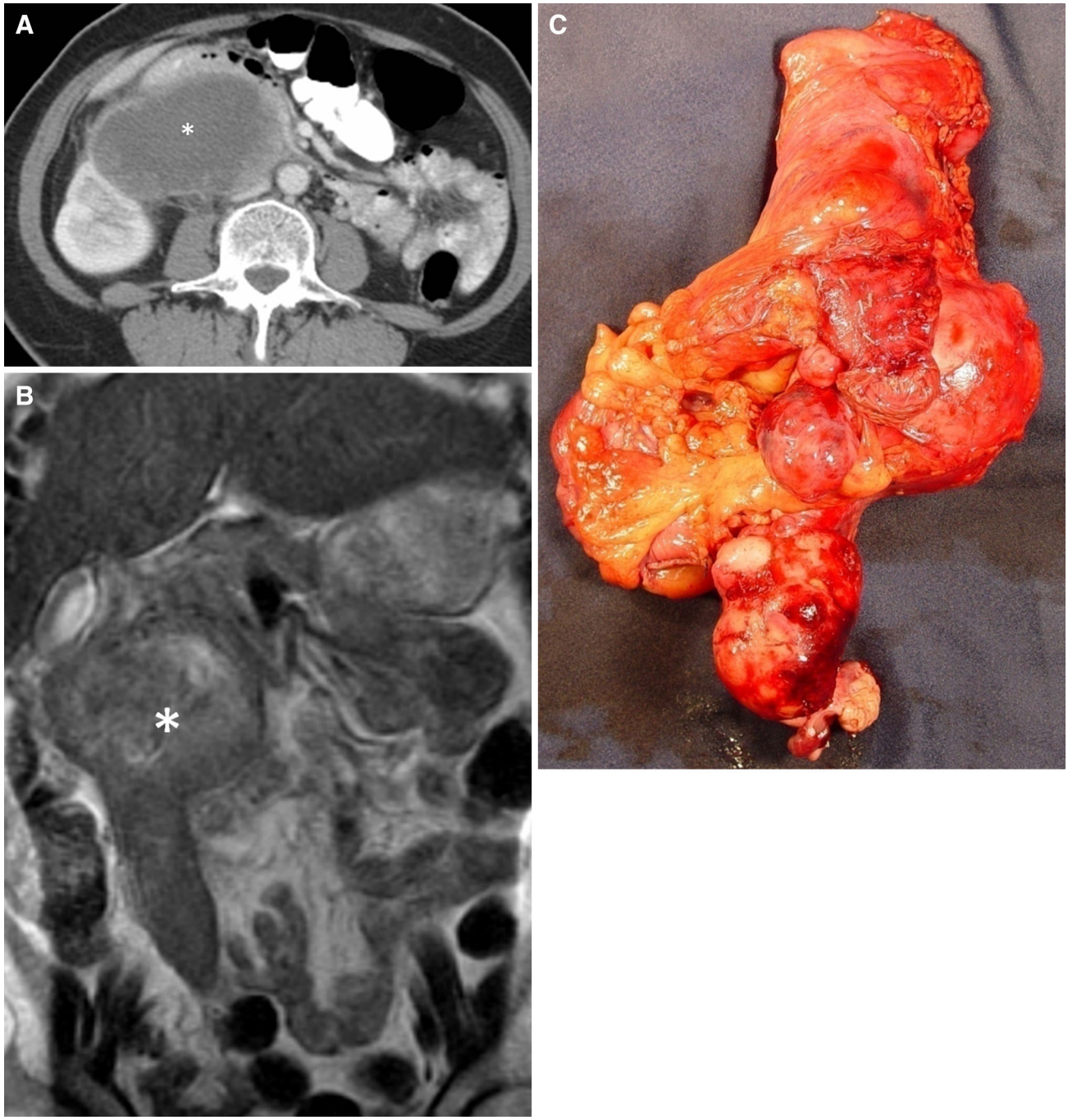

Fig. 6. Intravascular leiomyosarcomas. **A** Axial contrast-enhanced CT of the abdomen. **B** Coronal T2-weighted spin–echo MRI image. There is an extensive necrotic endoluminal mass expanding the right gonadal vein (*asterisk*). **C** Photograph of the gross specimen reveals a large well-defined lobulated mass occupying the right gonadal vein (*arrows*). Adherent omentum, bowel and ovary (*arrowhead*) are seen.

Lipoma

Lipomas are rare in the retroperitoneum (Fig. 10). A pure, fat-containing mass without enhancement or soft-tissue component (the hallmark picture for lipomas) is seen on imaging. Although the imaging characteristics of a retroperitoneal fatty mass may be suggestive of a benign lipoma, it is prudent to assume that the lesion represents a well-differentiated liposarcoma and should be treated accordingly [5].

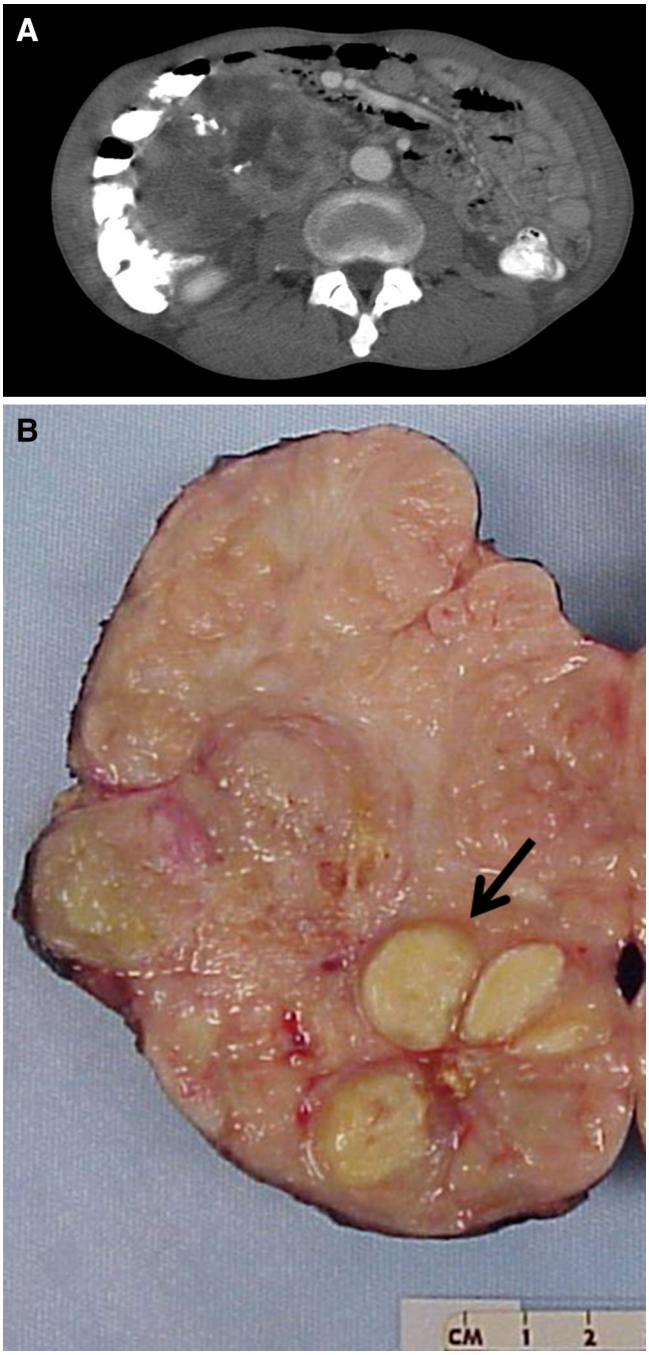

Fig. 7. Malignant fibrous histiocytoma. **A** Axial contrast-enhanced CT of the abdomen shows a large lobulated heterogeneous soft-tissue mass with areas of necrosis and coarse amorphous calcifications (*arrow*) located in the anterior pararenal space. This mass produces displacement of the bowel without mechanical obstruction. **B** Cut surface photograph of the gross specimen revealed fleshy areas mixed with necrotic foci. Focal areas of calcifications are noted (*arrow*).

Fig. 8. Alveolar rhabdomyosarcoma. Axial contrast-enhanced CT of the abdomen demonstrates an anterior pararenal space lobulated solid mass with areas of necrosis and heterogeneous enhancement (*asterisk*). The mass compresses the right kidney causing moderate hydronephrosis (*arrow*). The kidney shows delayed enhancement secondary to ischemic vascular defect due to parenchymal compression.

Leiomyoma

Commonly encountered in the uterus, leiomyomas rarely arise primarily from the retroperitoneum, yet occur almost exclusively in women. Many of these tumors histologically resemble uterine leiomyomas, have a low potential for recurrence and a good prognosis. Imaging findings are nonspecific and diagnosis is histopathological.

Angioleiomyoma (Fig. 11), also known as vascular leiomyoma, is an uncommon type of leiomyoma that originates from smooth muscle cells and contains thick-walled vessels. There are only a few cases of retroperitoneal angioleiomyoma reported in the literature. Since they are very uncommon, imaging characteristics of retroperitoneal angioleiomyomas are not well known. Uterine angioleiomyoma shows the areas of cystic degeneration and prominent tortuous vascular-like enhancing structures. Thus, angioleiomyoma should be included in the differential diagnosis when a retroperitoneal mass contains cystic components and prominent vascularization [12].

Neurogenic tumors

Neurogenic tumors constitute 10% to 20% of primary retroperitoneal tumors (Table 4) [1], occur in a younger age group than sarcomas, and are usually benign. These tumors can be classified as ganglion cell origin, paraganglionic system origin (pheochromocytomas, paragangliomas), or nerve sheath origin (neurilemmomas, neurofibromas, neurofibromatosis, and malignant nerve sheath tumors). Calcifications can occur in all types of neurogenic tumors [9]. Neurogenic tumors arise from sympathetic ganglia in the paraspinal region,

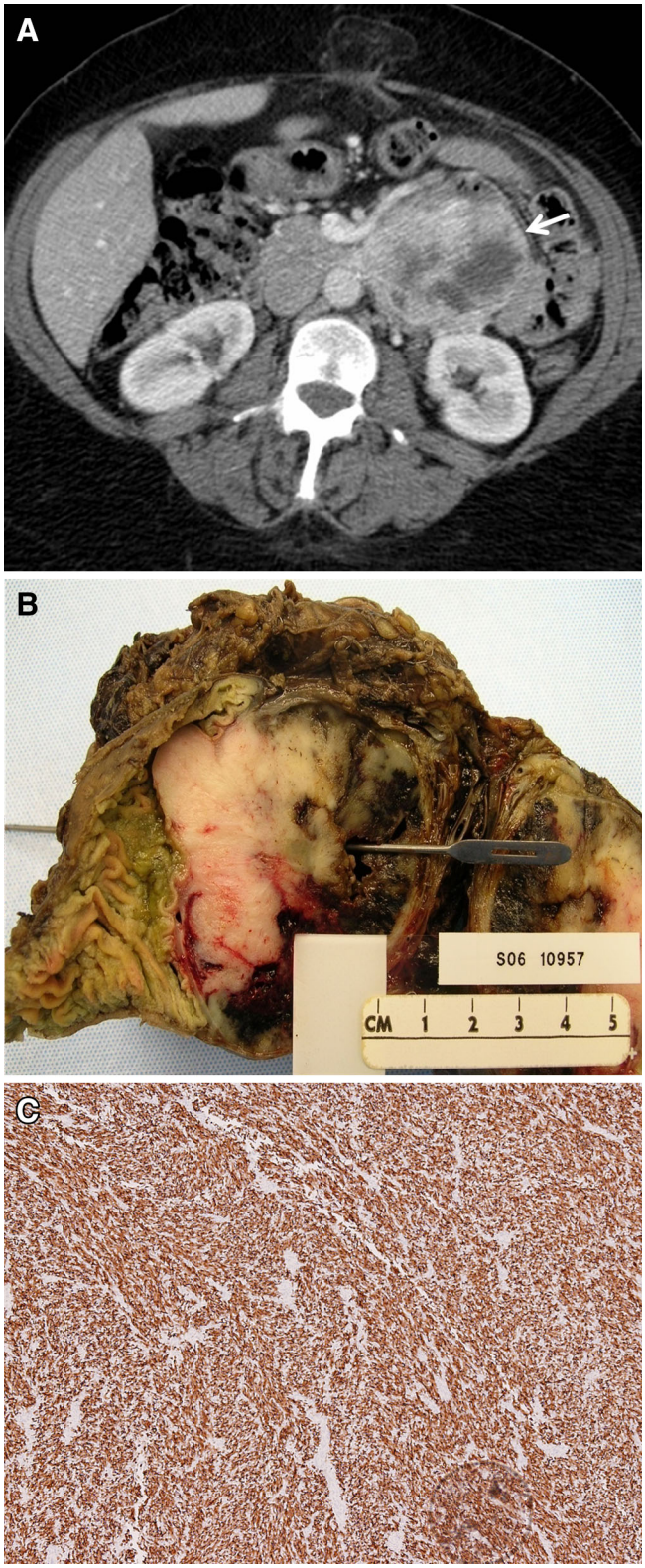

◀**Fig. 9.** Retroperitoneal benign GIST. **A** Axial contrast-enhanced CT abdomen shows a well-defined rounded retroperitoneal mass with heterogeneous enhancement due to central necrosis (*arrow*). **B** Photograph of the resected specimen of the GIST. There is a solid and partly hemorrhagic lesion in the duodenum wall, with intact and relatively normal overlying mucosa. **C** IHC staining demonstrates cellular spindle cell tumor strongly positive with CD117 (20× magnification).

adrenal medulla, or organ of Zuckerkandl, a body derived from neural crest located at the bifurcation of the aorta or at the origin of the inferior mesenteric artery. Occasionally neurogenic neoplasms originate from the urinary bladder, bowel wall, abdominal wall, and gallbladder [2, 9].

Tumors of ganglion cell origin

Tumors of ganglion cell origin include ganglioneuroma (benign), neuroblastoma (malignant), and ganglioneuroblastoma (intermediate). The adrenal gland is the most common primary site of involvement for these tumors. Neuroblastoma and ganglioneuroblastoma most often occur in infants and children, whereas ganglioneuroma tends to occur in adolescents and young adults [13].

Ganglioneuroma is a rare benign tumor that arises from the sympathetic ganglia. These tumors are composed entirely of ganglion cells and Schwannian stroma and do not contain neuroblasts, intermediate cells, or mitotic figures [13]. Malignant transformation is rare and the prognosis is excellent [1]. However, there are rare reports of metastasis [14]. This tumor is commonly seen in the 20- to 40-year-old group, with no sex predilection [2]. The retroperitoneum (32% to 52% of cases) and mediastinum (39% to 43% of cases) are the most common sites for ganglioneuroma, followed by the cervical region (8% to 9% of cases). In the retroperitoneum, the tumor is commonly seen along the paravertebral sympathetic ganglia (59% of cases) or, less commonly, in the adrenal medulla [2]. Ganglioneuromas range in size from 5 to 15 cm at presentation. Discrete punctate calcifications are seen in 20% to 30% of ganglioneuromas, unlike the coarse amorphous calcification of neuroblastomas. Necrosis and hemorrhage are uncommon. In CT, ganglioneuromas are well-circumscribed oval or lobular, often surrounding adjacent blood vessels without compressing the lumen. They are homogeneous and low attenuation on unenhanced CT scans with delayed heterogeneous enhancement. These features are

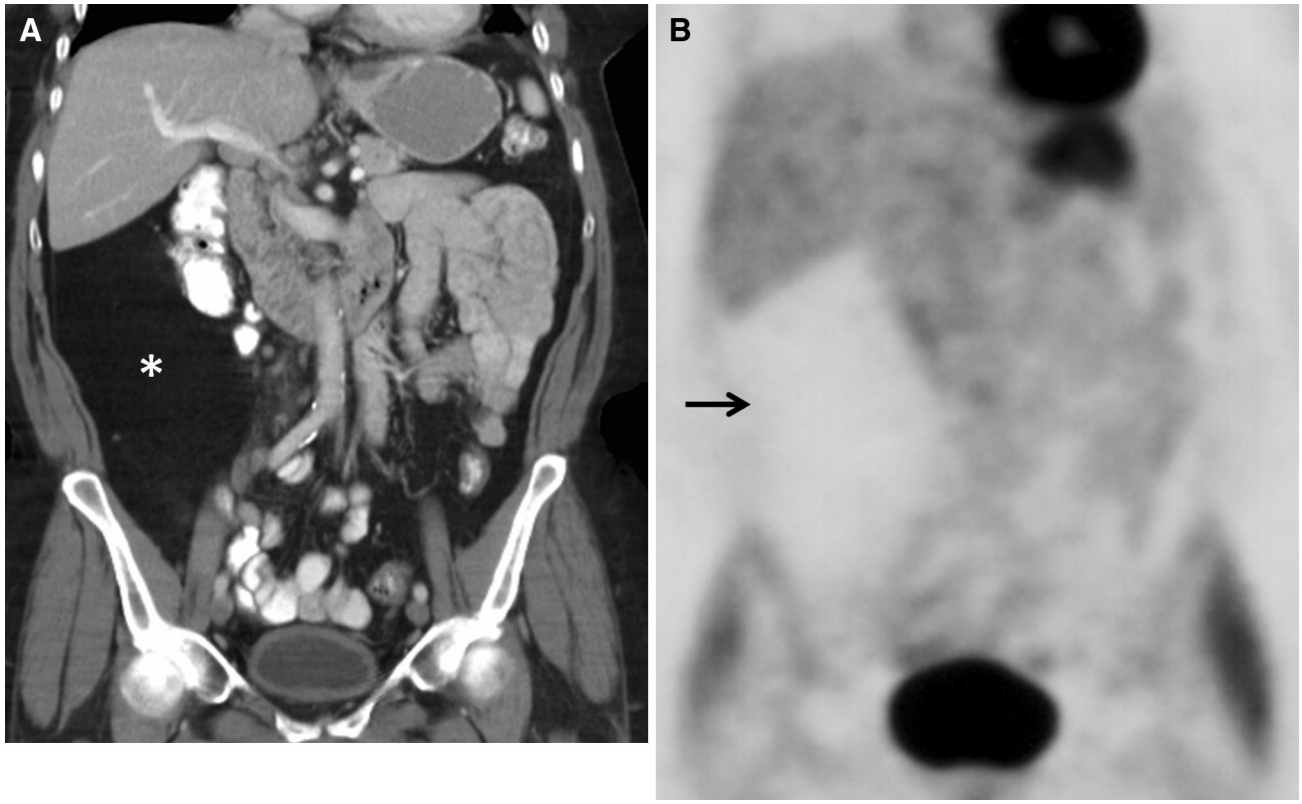

Fig. 10. Lipoma. Coronal contrast-enhanced CT abdomen (**A**) FDG-PET images (**B**) shows a homogeneous, well-circumscribed fat density mass in the right-sided retroperitoneum (*asterisk*). Leftward displacement of the duodenum and ascending colon is seen. FDG-PET image demonstrates a large area of photopenia (*black arrow*) corresponding to a retroperitoneal lipoma. Photopenia suggests minimal glucose metabolism in this region.

explained by an abundance of myxoid matrices in the tumors. On MR imaging, a ganglioneuroma is homogeneously hypointense on T1-weighted images, with varying signal intensity on T2-weighted images, depending on the myxoid, cellular, and collagen components [2, 5, 13, 14].

Ganglioneuroblastoma is an intermediate-grade tumor that has elements of benign ganglioneuroma and malignant neuroblastoma. At histologic analysis, they are malignant tumors that contain primitive neuroblasts and mature ganglion cells. The most common tumor site is the abdomen, followed by the mediastinum, neck, and lower extremities [13]. Ganglioneuroblastoma is a pediatric tumor occurring in the 2- to 4-year-old group, with no sex predilection, and it is rare in adults [2]. Imaging appearances vary ranging from a predominantly solid mass to a predominantly cystic mass with a few thin strands of solid tissue. These tumors may be partially or totally encapsulated and frequently contain granular calcification (Fig. 12) [13].

Neuroblastoma (Fig. 13) is a malignant tumor that is more commonly seen in males in their first decade of life. Two-thirds of neuroblastomas are located in the adrenal gland, and the remaining occurs along the paravertebral sympathetic chain [2]. On CT and MR imaging, a neuroblastoma is irregular, lobulated, and heterogeneous, and demonstrates coarse amorphous calcifications and variable contrast enhancement. Lesions may invade adjacent organs and encase vessels with luminal compression. Neuroblastomas tend to metastasize to bone, bone marrow, liver, lymph nodes, and skin [12]. As many as 70% of patients have metastatic disease at the time of diagnosis [2]. I-123 metaiodobenzylguanidine (MIBG) is the radiopharmaceutical used for evaluation of patients diagnosed with neuroblastomas. I-123 MIBG uptake can be seen in the primary tumor and the metastatic sites.

Tumors of the paraganglionic system

The paraganglionic system is composed of neural crest cells, which are found in the adrenal medulla, parasympathetic ganglia, and chemoreceptors. Tumors that arise from the chromaffin cells of the adrenal medulla are called pheochromocytomas, and those that arise in an extra-adrenal location (10%) are referred to as paragangliomas [2].

The rate of malignancy in paragangliomas is much higher, 22% to 50%, compared to 10% for

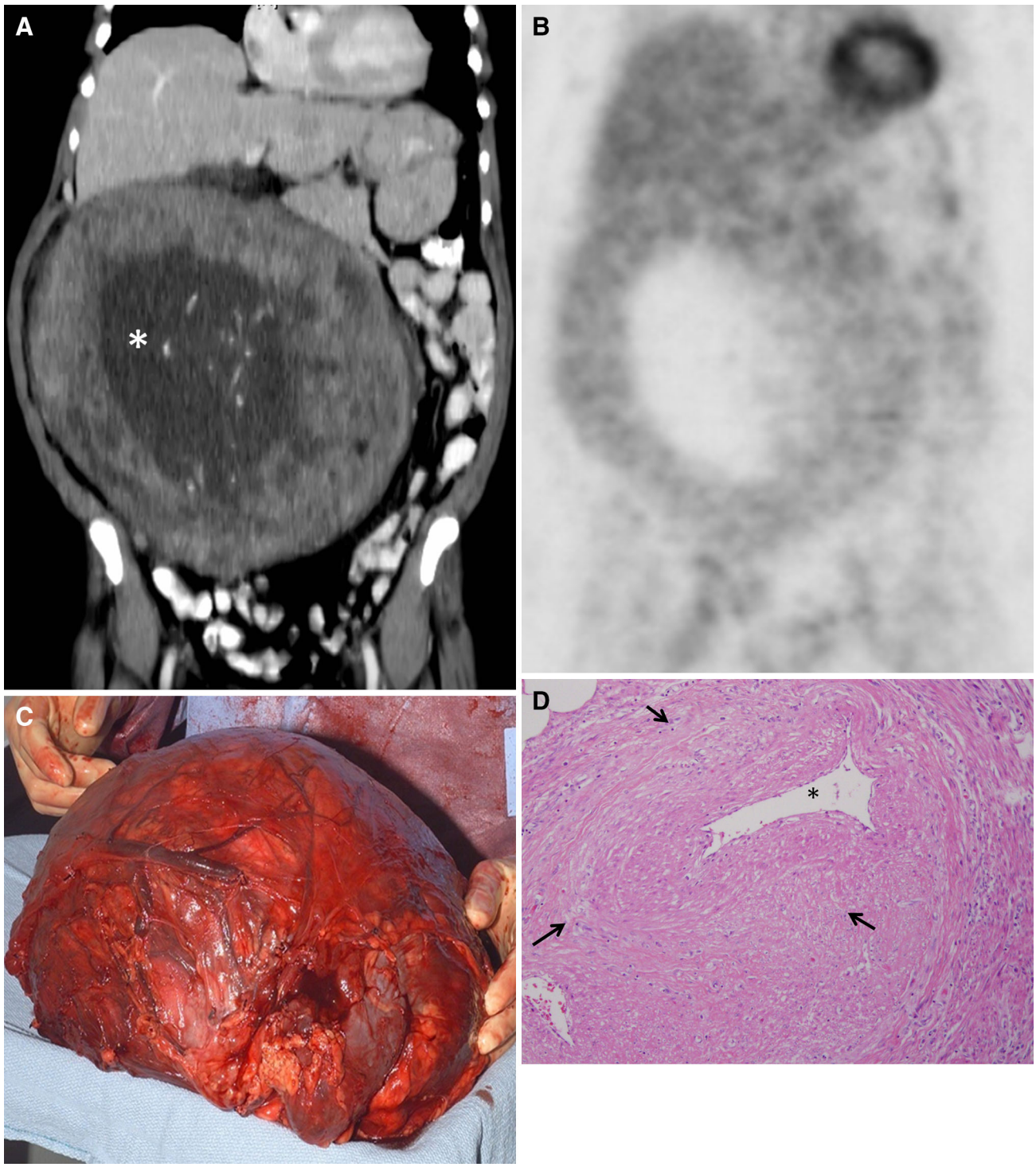

Fig. 11. Vascular leiomyoma. Coronal contrast-enhanced CT abdomen (**A**) and FDG-PET (**B**) demonstrates a large, oval, thick-walled mass with central necrosis (*asterisk* in **A**). Coronal PET image shows mild peripheral FDG activity (*arrow*), and central photopenia due to tumor necrosis (*arrowhead*). These findings suggest a low-grade malignancy. **C** Photograph of the gross specimen reveals a large encapsulated mass (810 g) with prominent dilated peripheral vessels compressing but not involving the kidney and intestines. The cut surfaces are whorled in appearance with spongy areas and foci of cystic degeneration. The compressed surrounding retroperitoneal adipose tissue shows vascular congestion and lymphangiectasia (dilated lymphatics) (**D**). Photomicrograph (H–E stain) demonstrates thick-walled vessel (*asterisk*) with surrounding benign smooth muscle proliferation (*arrows*).

Table 4. Neurogenic tumors: characteristic imaging findings and other diagnosis features

Neurogenic tumors	Image finding	Other diagnosis features
Ganglioneuroma	Homogeneous paravertebral mass. Extension along normal structures. Delayed enhancement	20–40 years age group, with no sex predilection
Ganglioneuroblastoma	Vary ranging from a predominantly solid mass to a predominantly cystic mass. Encapsulated. May contain granular calcification	2–4 years age group, with no sex predilection
Neuroblastoma	Irregular, lobulated, heterogeneous. 85% calcifications (coarse, amorphous, mottled). Variable contrast enhancement	Males, 1st decade of life
Paragangliomas	Paravertebral mass, intense early enhancement. 40% central necrosis. 15% punctate calcification. Fluid–fluid level	High catecholamine levels, hypertension
Schwannomas	Oval mass that frequently demonstrates prominent cystic degeneration and calcification	Female predilection. 20–50 years. Encapsulated. Compression of nerve to one side
Neurofibroma	Well-circumscribed, round mass with homogeneous contrast enhancement. Occasionally, myxoid degeneration	Male predilection. 20–40 years (younger in NF1). Usually unencapsulated. Diffuse expansion of the entire nerve
Plexiform neurofibroma	Bilaterally symmetric, elongated paraspsoas masses with homogeneous low attenuation	Is characteristic of NF-1

pheochromocytomas [1]. Pheochromocytomas have been called ''ten percent tumors,'' because approximately 10% are bilateral, 10% are extra-adrenal (paragangliomas of the retroperitoneum, mediastinum, or urinary bladder), 10% occur in children, 10% are familial, 10% are malignant, and 10% are not associated with hypertension [13]. In the retroperitoneum, 40% of paragangliomas produce high catecholamine levels that result in hypertension and elevated urinary metanephrine or vanillylmandelic acid levels [2, 5]. Rarely, paraganglioma can manifest with acute abdomen caused by retroperitoneal hemorrhage [2]. Paraganglioma can be associated with type 1 neurofibromatosis, multiple endocrine neoplasia syndrome, and von Hippel–Lindau syndrome. They are commonly seen in the third to fourth decades of life, with no sex predilection. In the retroperitoneum, the most common site for a paraganglioma is the organ of Zuckerkandl (Fig. 14).

On CT, paragangliomas are usually 3 cm or larger, well-marginated, round, and lobular tumors in a paraaortic location. They are usually highly vascular tumors demonstrating intense early enhancement (Fig. 15). Central necrosis occurs in approximately 40%, and (Fig. 16) punctate calcification can be seen in approximately 15% [1]. Malignant lesions tend to be larger with more irregular margins and more extensive necrosis. If no lesion is found or identified on CT and laboratory test results remain positive, radionuclide imaging with metaiodobenzylguanidine is suggested to identify the occult lesion [13]. On MR imaging, they are heterogeneously bright on T2-weighted imaging, though less than 80% of paragangliomas show the characteristic uniform high signal on T2-weighted imaging (caused by the hemorrhage within the tumor). Hemorrhagic portions can be bright on T1-weighted sequences, and fluid–fluid levels may be seen [15].

Tumors of nerve sheath origin

Tumors of nerve sheath origin include schwannoma (also known as neurilemoma), neurofibroma, neurofibromatosis, and neurogenic sarcoma (malignant schwannoma). More than 90% of these tumors are benign. The benign lesions are identified in young and middle-aged adults [13].

Schwannoma, or neurilemoma, is a benign tumor that arises from the perineural sheath of Schwann (neurilemma) [2]. Schwannoma accounts for 6% of retroperitoneal neoplasms, comprising approximately 3% of all schwannomas [2, 16]. They are usually asymptomatic and are more common in females (2:1), particularly in the 20-to 50-year-old age group [2]. Retroperitoneal schwannomas are usually solid encapsulated tumors that are commonly located in the paravertebral region and, less commonly, adjacent to the kidney, pre-sacral space, and abdominal wall [2]. They are usually larger and have a higher tendency to undergo spontaneous degeneration and hemorrhage compared with their counterparts arising in the head and neck or extremities, which are usually solid and small [16]. These tumors are usually asymptomatic and are thought to be slow growing. Malignant

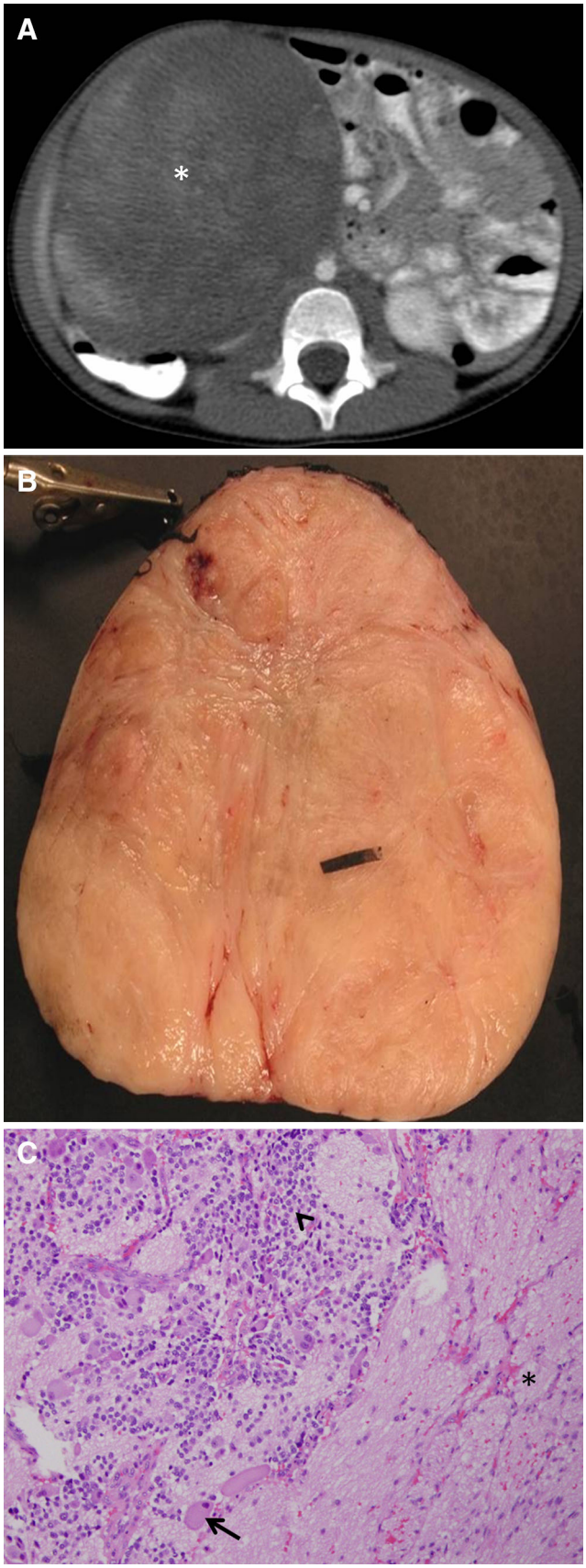

◀**Fig. 12.** Ganglioneuroblastoma in a 3-year-old female. **A** Axial contrast-enhanced CT abdomen shows a large, round, well-defined cystic appearing mass on the right-sided retroperitoneum (*asterisk*). **B** Photograph of the gross specimen reveals a large ovoid rubbery thinly encapsulated mass (518 g). Cut surface shows tan, multilobulated firm appearance with foci of hemorrhage and calcification. **C** Photomicrograph (200×; H–E stain) demonstrates ganglion cells (*arrow*), which are cells with abundant cytoplasm, rounded contour, and large nuclei. Neuroblasts, which are the dark purple cells with scant cytoplasm (*arrowhead*), and neuropil, which is the fine, fibrillary light pink-staining material (*asterisk*).

transformation is rare [2]. On CT, a schwannoma appears as a well-demarcated round or oval mass that frequently demonstrates prominent cystic degeneration and or calcification, which can be punctate, mottled, or curvilinear.

The nerve of origin is often difficult to identify. On MR imaging, cellular areas are hypointense on T1- and T2-weighted images. Cystic areas appear hyperintense on T2-weighted images. After contrast enhancement, schwannomas demonstrate variable homogeneous or heterogeneous enhancement, representing a variable histologic composition, which includes cellular areas adjacent to myxoid regions, cystic degeneration, xanthomatous change, or collagen deposition [1].

Neurofibroma is a benign nerve sheath tumor composed of nerve sheath cells intermingled with thick collagen bundles with a small to moderate amount of myxoid degeneration [1]. Cystic degeneration is rare [2]. Neurofibromas only account for about 1% of retroperitoneal tumors [1]. They are solid, usually superficial tumors, and occur most often in patients 20–40 years. In patients with a solitary neurofibroma, 30% will eventually be diagnosed to have neurofibromatosis type 1 (NF-1) [1].

Unlike schwannomas, which displace the nerve fibers, the nerve fibers in neurofibromas transverse the tumor [1]. Malignant degeneration is more common with neurofibromas than with schwannomas, particularly in those patients who have neurofibromatosis [2]. On CT, a neurofibroma is depicted as a well-defined round, homogeneously hypoattenuating lesion (20–25 HU) (HU = Hounsfield unit) because of the presence of lipid-rich Schwann cells and adipocytes and the entrapment of adjacent fat. Typically, there is homogeneous contrast enhancement (30–50 HU) that is due to collagen bands, but cystic areas caused by myxoid degeneration may also be seen.

On T1-weighted images, the central portion of the tumor shows higher signal intensity due to the neural tissue component, and on T2-weighted images, the periphery has higher signal intensity due to the myxoid

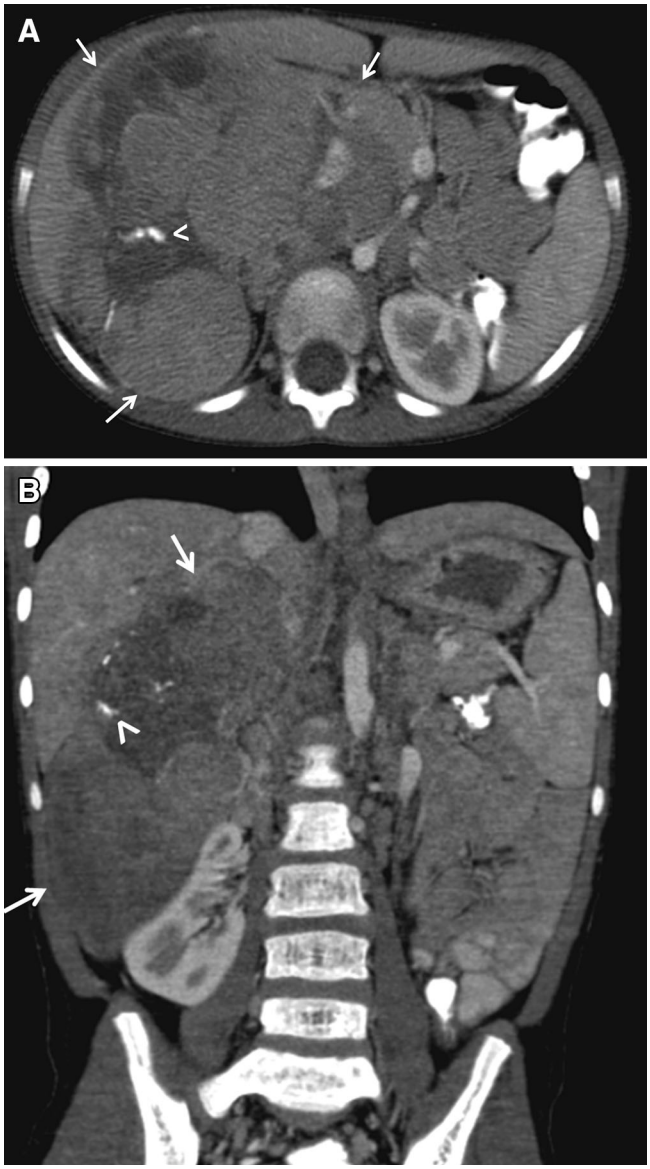

Fig. 13. Neuroblastoma in a 6-year-old male. Axial (**A**) and coronal (**B**) contrast-enhanced CT of the abdomen demonstrates a lobulated heterogeneous soft-tissue mass with areas of necrosis in the right perinephric space (*arrows*). There is also coarse amorphous calcifications (*arrowhead*) and variable contrast enhancement. The lesion produces compression and inferior displacement of the ipsilateral kidney.

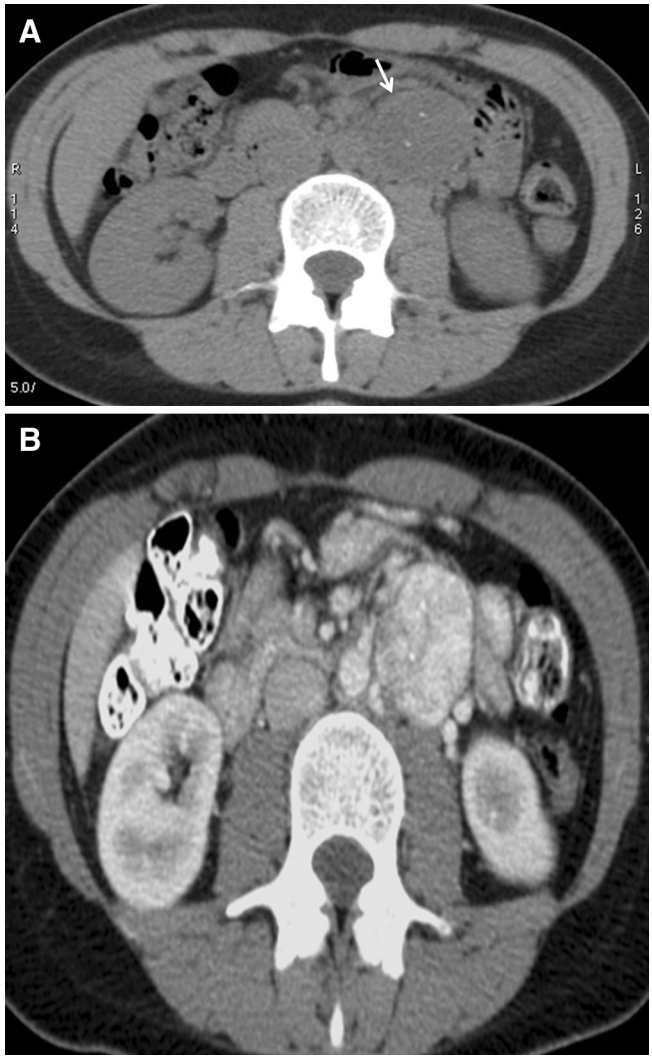

Fig. 14. Paraganglioma. **A** Axial unenhanced CT abdomen shows a well-marginated, low density tumor (*arrow*) with intralesional punctate calcifications in the left para-aortic space consistent with a paraganglioma in the organ of Zuckerkandl. **B** Axial contrast-enhanced CT image shows typical intense early enhancement of the mass.

degeneration. Tumors involving the neural foramen have a dumbbell shape with expansion of the bone foramina or vertebral body scalloping.

Plexiform neurofibroma (PN) is an interdigitating network of fronds of tumor occurring along a nerve and its branches. PN is characteristic of NF-1, and fulfills one of the two criteria required for the diagnosis of NF-1 (nearly all patients with PN will have NF-1) [18]. Although PN can occur in a variety of locations within the body, the involvement of the retroperitoneal space and pelvis is uncommon [17]. Unlike most primary retroperitoneal neoplasms, the CT features of most PN are sufficiently characteristic that a specific diagnosis usually can be made without invasive procedures [18]. CT demonstration of bilaterally symmetric, elongated para-psoas masses with homogeneous low attenuation indicates a benign retroperitoneal PN. If not clinically known, the diagnosis of NF-1 should be suggested [18]. When bilateral lesions are present, asymmetry in axial diameter and an asymmetric attenuation pattern should raise the suspicion of malignant transformation. If the bilateral para-psoas masses differ in size more than 2 cm or attenuation on CT, the larger lesion might represent a malignant change and should be biopsied [17]. F-18 FDG-PET/CT has been shown to be very sensitive and

◀**Fig. 15.** 50-year-old white male with a primary retroperitoneal paraganglioma simulating a pancreatic mass. **A** Axial contrast-enhanced CT abdomen shows a hypervascular retroperitoneal solid mass (*arrow*). **B** Curved multiplanar reconstruction demonstrates a close contact of the paraganglioma with the proximal pancreas (*arrowhead*). Pancreatic body and tail show parenchymal atrophy and ductal dilatation. **C** Fused transaxial PET/CT image showing intense FDG activity in the retroperitoneal mass (*crosshairs*).

specific imaging modality for the diagnosis of malignant peripheral nerve sheath tumors in patients with neurofibromatosis type 1 [9].

On MRI, PN are seen as low-signal intensity lesions on T1-weighted images with a signal intensity slightly greater than the surrounding muscles. On T2-weighted images they are markedly hyperintense. Multiple hypointense septations can be seen within the tumor on T2-weighted images [17].

Malignant nerve sheath tumors (MNST) (Fig. 17) are rare tumors that account for approximately 3% to 10% of all soft-tissue sarcomas [19]. They are aggressive high-grade neoplasms with a poor prognosis [4]. MNST include malignant schwannoma, neurogenic sarcoma, and neurofibrosarcoma. Fifty percent (50%) of these tumors originate de novo, and the rest of them are derived from neurofibroma or ganglioneuroma or occur after exposure to radiation [2]. They have a tendency to recur locally, and distant metastases occur at a rate of 65% [4]. MNST are more common in the 20- to 50-year-old group, with no sex predilection [2]. In 25% to 50% of cases, these tumors are associated with NF-1. Having an NF-1 is considered as the most important risk factor for developing malignant peripheral nerve sheath tumors [19]. Imaging criteria are unreliable in differentiating malignant from benign nerve sheath tumors [13]. On imaging, malignant nerve sheath tumors are vascular masses closely associated with neurovascular bundles. Useful characteristics for distinguishing between malignant peripheral nerve sheath tumors and neurofibromas include increased largest dimension of the mass, presence of peripheral enhanced pattern, presence of peri-lesional edema like zone, and presence of intra-tumoral cystic lesions. The presence of two to four of these features is suggestive of malignancy (sensitivity, 61%; specificity, 90%) [19].

Germ cell, sex cord, and stromal cell tumors

Extragonadal germ cell tumor

Although germ cell tumors are seen most commonly in the testes or ovaries, 1% to 2.5% of germ cell tumors originate in an extragonadal location (Table 5) [2]. Primary extragonadal germ cell tumors (PEGCT) are rare, accounting for approximately 5% of all primary retroperitoneal tumors. This is the second most common site for PEGCT after the mediastinum [4]. They almost exclusively occur in males with peak incidence in the fifth

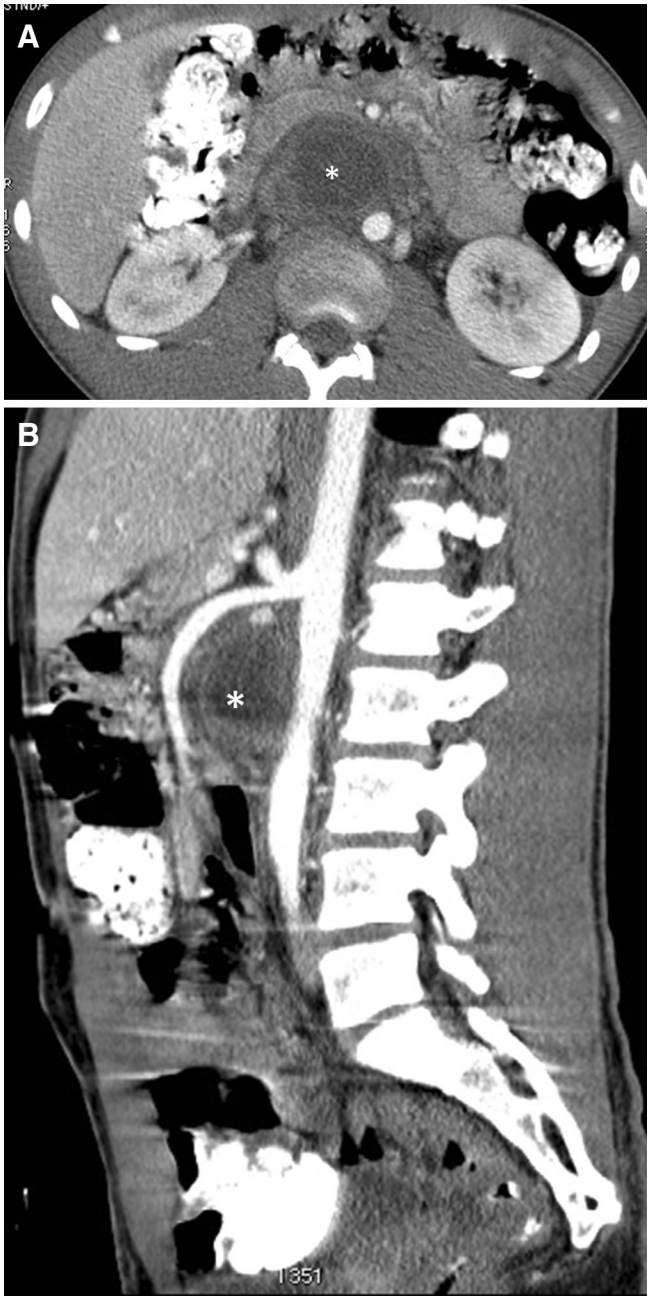

Fig. 16. Atypical retroperitoneal paraganglioma. **A** Axial and **B** sagittal contrast-enhanced CT abdomen show a well-marginated hypodense lesion with central necrosis (*asterisk*) located in the retroperitoneum between de aorta, superior mesenteric artery and the IVC.

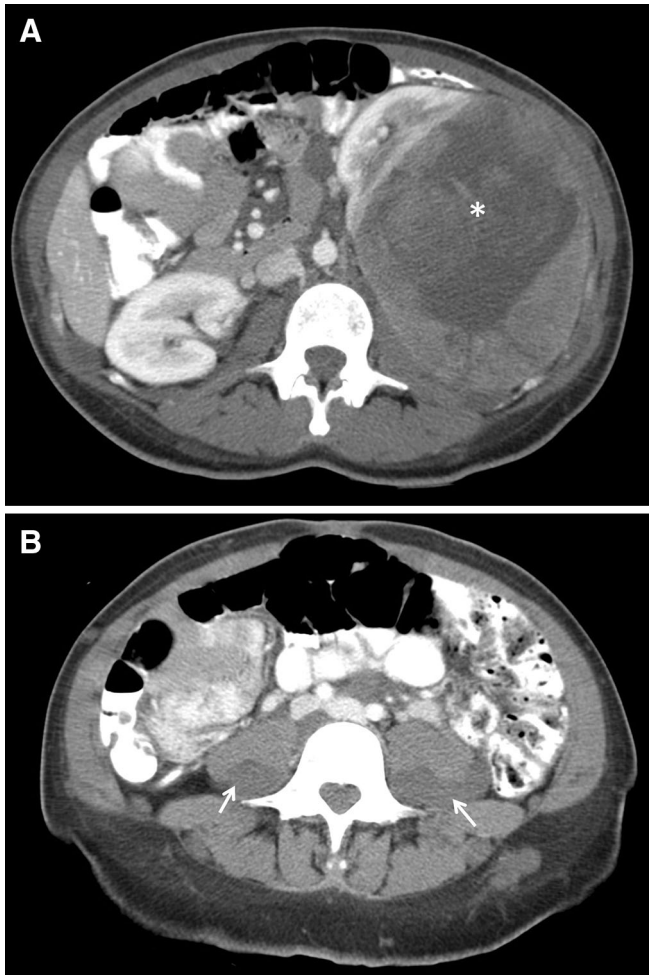

Fig. 17. A 29-year-old African–American female with malignant peripheral nerve sheath tumor (MPNST). Axial contrast-enhanced CT abdomen shows (**A**) a large, oval, well-defined necrotic mass located in the left perinephric space consistent with MPNST (*asterisk*). **B** Bilateral and symmetric low-attenuation masses are noted in psoas regions consistent with benign peripheral nerve sheath tumor (*arrows*).

decade of life [4]. They are believed to arise from primordial germ cell rests that have failed to migrate during the fourth to sixth week of embryonic development [20].

The majority of retroperitoneal germ cell tumors represents metastases from primary testicular neoplasms (retroperitoneal metastasis is seen in 30% of gonadal tumors, and therefore, careful examination of the testes is crucial). The basic histologic types are seminoma; embryonal carcinoma; choriocarcinoma; teratoma with mature, immature, or malignant foci; and yolk sac tumor. Elevated levels of alpha-fetoprotein are seen in embryonal carcinoma and yolk sac tumor, whereas elevated levels of the beta subunit of human chorionic gonadotropin are seen in choriocarcinoma [4].

On imaging, the findings for PEGCT are nonspecific. Retroperitoneal germ cell tumors typically appear as a large midline lobular mass of heterogeneous CT attenuation or MR signal intensity. A midline mass is more suggestive of a PEGCT than of metastasis [2]. Seminomas and embryonal carcinomas may appear homogenous. Areas of hemorrhage and necrosis may also be seen, especially with nonseminomatous germ cell tumors [4]. Calcifications, tooth-like or well-defined, and fat can be seen very frequently in teratomas [2]. A pathognomonic finding in teratomas is the presence of a fat-fluid level and chemical shift between fat and fluid [2].

Table 5. Extragonadal germ cell tumors: characteristic imaging findings and other diagnosis features

Extragonadal germ cell tumors	
Image finding	Other diagnosis features
• Large midline lobular masses of heterogeneous CT attenuation or MR signal intensity • Seminomas and embryonal carcinomas may appear homogenous	• Elevated levels of alpha-fetoprotein are seen in embryonal carcinoma and yolk sac tumor • Elevated levels of the beta subunit of human chorionic gonadotropin are seen in choriocarcinoma
• Areas of hemorrhage and necrosis may be seen, especially with nonseminomatous germ cell tumors • Calcification (tooth-like or well defined) and fat can be seen in 56% and 93% of teratomas • A fat-fluid (sebum) level and chemical shift between fat and fluid are pathognomonic for teratomas • Large midline lobular masses of heterogeneous CT attenuation or MR signal intensity • Seminomas and embryonal carcinomas may appear homogenous	• The majority of retroperitoneal germ cell tumors represent metastases from primary testicular neoplasms • Elevated levels of alpha-fetoprotein are seen in embryonal carcinoma and yolk sac tumor • Elevated levels of the beta subunit of human chorionic gonadotropin are seen in choriocarcinoma

Primary sex cord stromal tumors

These tumors are extremely rare and are seen in women over a wide age range (30–76 years). Extra-ovarian primary sex cord stromal tumors arise from ectopic sex cord stromal tissues or from the sex cord—like the differentiation of somatic cells. These tumors are more commonly seen in the pelvis along the broad ligament or fallopian tubes and, less commonly, in the retroperitoneum or adrenal glands. Most of these tumors are granulosa cell tumors [2].

Adult granulosa cell tumors (Fig. 18) are estrogen producing tumors that occur predominantly in peri- and postmenopausal women. Granulosa cell tumors can arise in locations other than the ovary and may be derived from the mesenchyme of the genital ridge. Women who have undergone oophorectomy may have the potential to develop granulosa cell tumors. The locations of these tumors have been described as the broad ligament, retroperitoneum, and adrenal glands. The imaging findings are nonspecific. CT and MR images show heterogeneous solid tumors, with heterogeneous enhancement [2, 21].

Lymphomas

Lymphomas constitute roughly one-third of all primary retroperitoneal neoplasms. Hodgkin's lymphoma (HD) has a bimodal age distribution and peaks in the early 20s. It usually presents with limited disease spread (stage I or II). Extranodal sites are usually not involved. Non-Hodgkin's lymphoma (NHL) presents in patients 40–70 years of age, often already in an advanced disease stage (stage III or IV) upon diagnosis. Extranodal disease in NHL is much more common than in HD. Para-aortic lymph nodes are involved in 25% of patients with HD and 55% of patients with NHL. Bone marrow involvement at presentation occurs in more than 40% of patients with NHL. On imaging, a lymphoma typically appears as a well-defined homogeneous and mildly enhancing para-aortic or pelvic mass that extends between structures without compressing them. Necrosis and calcification are very uncommon [1, 4]. Intensely increased FDG uptake on the PET-FDG scan is noted in the areas of the pelvic and retroperitoneal lymphatic pathways, which correlates with areas of lymphadenopathy evident on CT scan [9].

Primary non-neoplastic retroperitoneal lesions

Retroperitoneal fibrosis

Retroperitoneal fibrosis (RF) encompasses a range of diseases characterized by proliferation of aberrant fibro-inflammatory tissue, which usually surrounds the infrarenal portion of the abdominal aorta, inferior vena cava, and iliac vessels. It may extend to neighboring structures. In about 56% to 100% of patients with idiopathic RF, the fibro-inflammatory tissues entrap the ureters and cause obstructive uropathy and subsequent renal failure.

Ureteral involvement is most often bilateral and leads to renal failure. RF is typically idiopathic ($>70\%$ of cases). Although in the rest of the cases ($<30\%$), RF is found to be secondary to factors that include drug use (derivatives of ergot alkaloids), malignancies (lymphoma, RS, carcinoid tumor, and metastatic disease from primary cancers of the stomach, colon, breast, lung, genitourinary tract, or thyroid gland), infections (histoplasmosis, tuberculosis, actinomycosis), radiation therapy, major trauma, major abdominal surgeries, retroperitoneal hemorrhage or hematoma, and proliferative diseases (Erdheim–Chester disease and other histiocytoses). Although retroperitoneal fibrosis manifests as an isolated retroperitoneal disease, it can also be associated with other fibrosing conditions, such as sclerosing cholangitis, Riedel thyroiditis, fibrotic pseudotumor of the orbit, and autoimmune pancreatitis, all of which

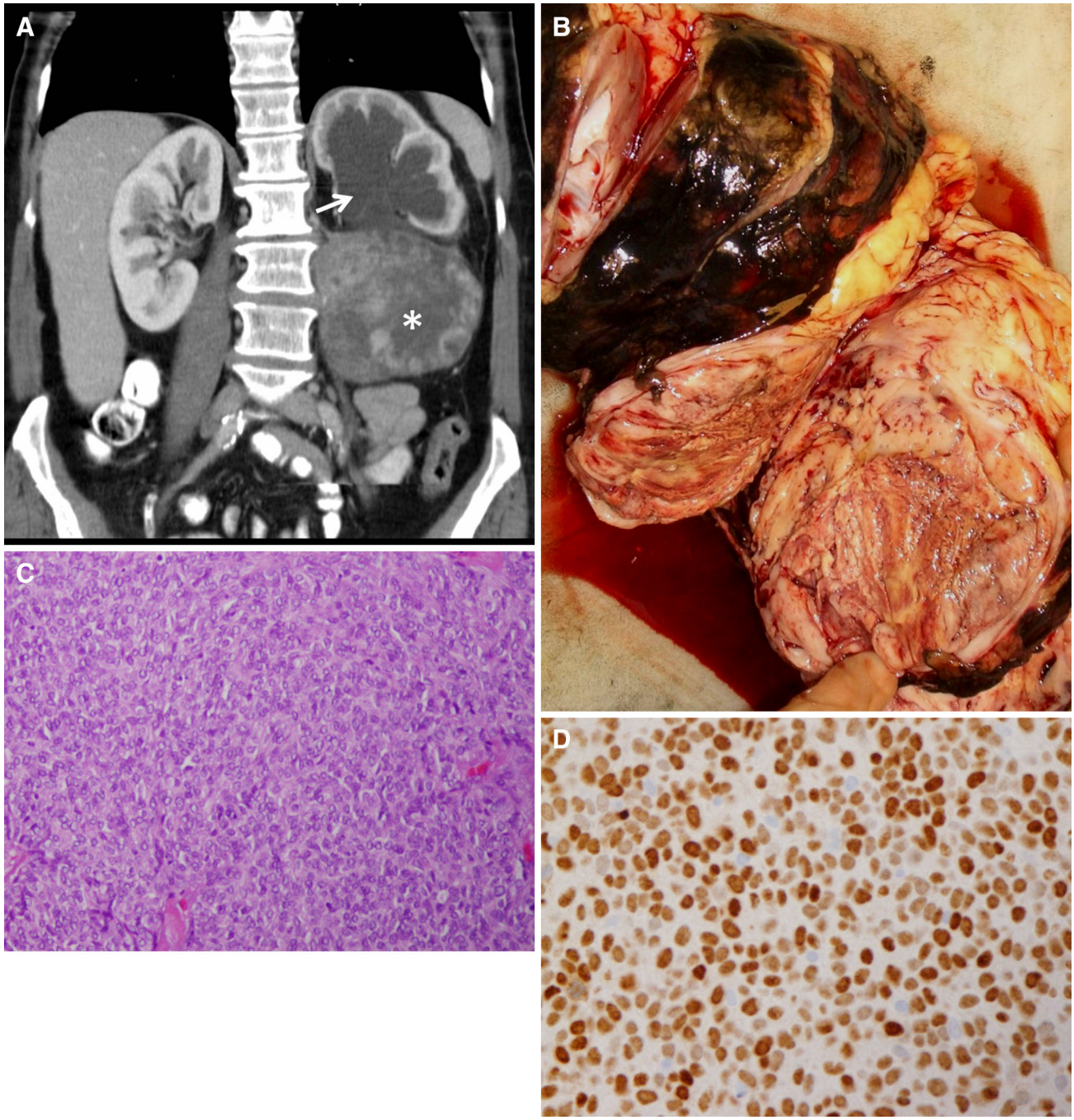

Fig. 18. Adult granulosa cell tumor. **A** Coronal contrast-enhanced CT abdomen shows a round, well-defined mass with heterogeneous enhancement, located in the left perinephric space (*asterisk*). This lesion produces compression of the left ureter causing proximal hydronephrosis (*arrow*). **B** Photograph of the gross specimen reveals a circumscribed thinly encapsulated mass with fleshy solid areas, foci of cystic degeneration, and yellow areas of necrosis. **C** Photomicrograph (H&E, 200×) shows sheets of round to oval tumor cells with Call–Exner bodies (this is formed by a discrete array of granulosa cells with angular grooved nuclei and central inspissated eosinophilic material). **D** Tumor cells are strongly positive for estrogen receptor.

form part of the group labeled "multifocal fibrosclerosis." If promptly diagnosed and treated, idiopathic and most other benign forms of RF have a good prognosis. In contrast, malignant RF, which accounts for up to 10% of cases, has a poor prognosis. Idiopathic RF is more common in males (3:1), particularly in the 40- to 60-year-old group [2, 22].

RF consist of a well-delimited but irregular soft-tissue peri-aortic mass that extends from the level of the renal arteries to the iliac vessels and often progresses through the

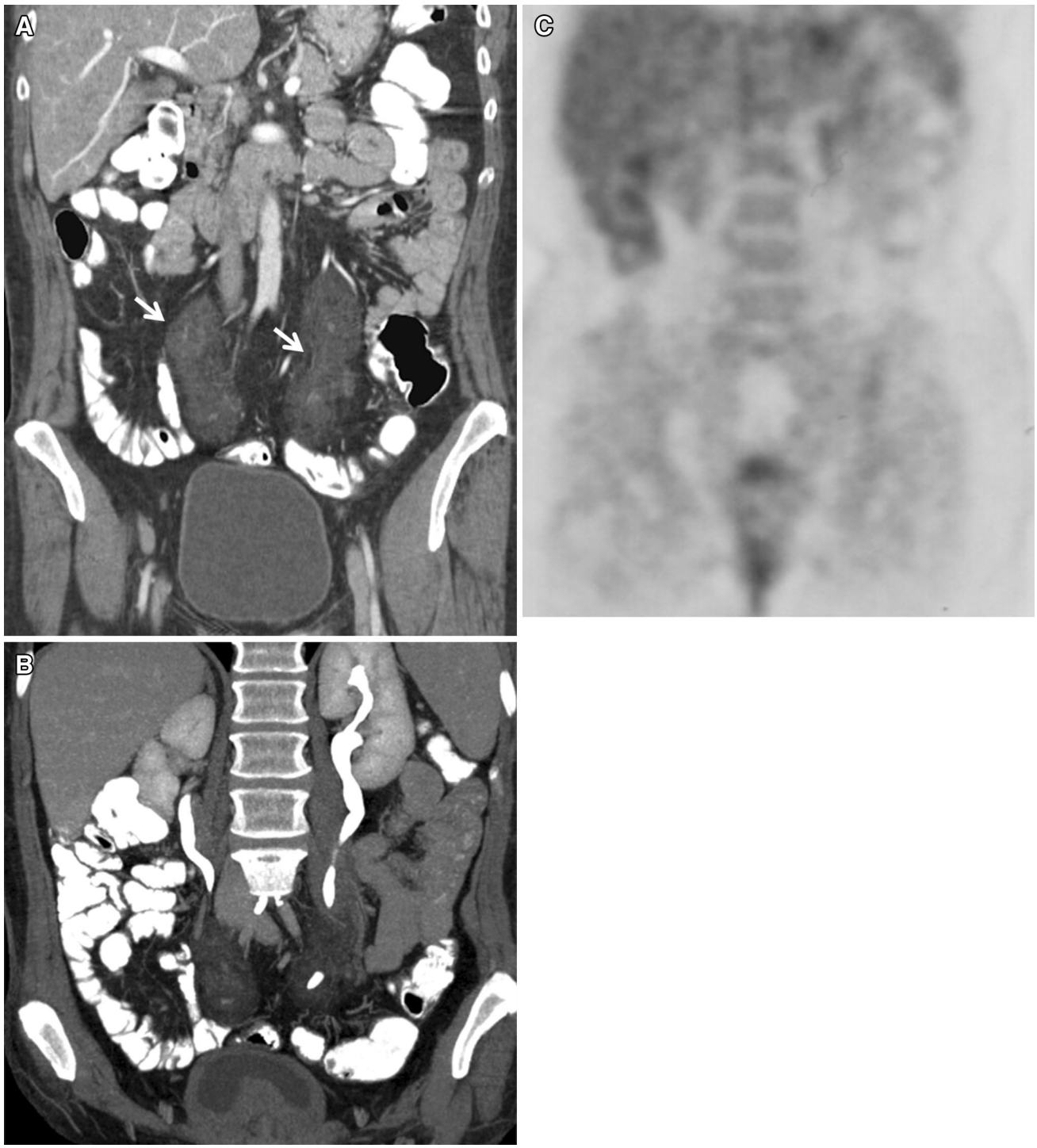

Fig. 19. Retroperitoneal fibrosis. **A** Coronal contrast-enhanced CT abdomen shows an ill-defined low density mass in the peri-aortic and pericaval spaces (*arrows*). **B** Coronal maximum intensity projection reconstruction during excretory phase CT abdomen demonstrates mild bilateral hydronephrosis secondary to distal encasement of both ureters. **C** Coronal PET scan image shows faint FDG uptake of the mass.

retroperitoneum to envelop the ureters and inferior vena cava (Fig. 19). The mass usually lies anterior and lateral to the aorta, so it does not displace the aorta and IVC anteriorly, as lymphoma or metastatic nodes often do. Avid enhancement is seen in the active stages of retroperitoneal fibrosis, with little or no enhancement in the chronic phase. MR imaging shows high-signal intensity on T2-weighted images in the acute phase of the disease,

and low-signal intensity in the chronic fibrosing phase. The FDG-PET scan shows increased uptake of FDG in the retroperitoneal space and is useful for detecting metabolic activity and distant disease. A lack of radiotracer uptake in the mass on FDG-PET imaging indicates a metabolically inactive disease. Due to its low specificity, 18F-FDG-PET is not useful for diagnosis of idiopathic and other benign forms of RF. Furthermore, FDG uptake in the aortic wall is nonspecific for RF and can also occur in elderly patients, especially those with hyperlipidemia and a history of cardiovascular disease [2, 22].

Conclusions

Primary retroperitoneal neoplasms are notable for their widely disparate histologies and presentations. While a specific diagnosis of a retroperitoneal malignancy can be challenging due to an overlap of imaging findings, CT and MR imaging can demonstrate important characteristics of these tumors. Combined with clinical and demographic information, CT and MR imaging may help in narrowing the differential diagnosis.

Compliance with ethical standards

Conflict of Interest Guillermo P. Sangster, Matias Migliaro, Maureen G. Heldmann, Peeyush Bhargava, Alireza Hamidian, and Jaiyeola Thomas-Ogunniyi declare that they have no conflict of interest.

Ethical approval All procedures performed in studies involving human participants were in accordance with the ethical standards of the Institutional and/or National Research Committee and with the 1964 Helsinki declaration and its later amendments or comparable ethical standards.

References

1. Neville A, Herts BR (2004) CT characteristics of primary retroperitoneal neoplasms. Crit Rev Comput Tomogr 45(4):247–270
2. Rajiah P, Sinha R, Cuevas C, et al. (2011) Imaging of uncommon retroperitoneal masses. RadioGraphics 31:949–976
3. Francis IR, Cohan RH, Varma DGK, Sondak VV (2005) Retroperitoneal sarcomas. Cancer Imaging 5:89–94
4. Osman S, Lehnert BE, Elojeimy S, et al. (2013) A comprehensive review of the retroperitoneal anatomy, neoplasms, and pattern of disease spread. Curr Probl Diagn Radiol 42(5):191–208
5. Craig WD, Fanburg-Smith JC, Henry LR, Guerrero R, Barton JH (2009) From the archives of the AFIP. Fat-containing lesions of the retroperitoneum: radiologic–pathologic correlation. RadioGraphics 29:261–290
6. Nishino M, Hayakawa K, Minami M, et al. (2003) Primary retroperitoneal neoplasms: CT and mr imaging findings with anatomic and pathologic diagnostic clues. RadioGraphics 23:45–57
7. Scali E, Chandler T, Heffernan E, et al. (2015) Primary retroperitoneal masses: what is the differential diagnosis? Am J Roentgenol 40(6):1887–1903
8. Kim EY, Kim SJ, Choi D, et al. (2008) Recurrence of retroperitoneal liposarcoma: imaging findings and growth rates at follow-up CT. Am J Roentgenol 191:1841–1846
9. Kitajima K, Kono A, Konishi J, et al. (2013) 18F-FDG-PET/CT findings of retroperitoneal tumors: a pictorial essay. Jpn J Radiol 31:301–309
10. Casella C, Villanacci V, D'Adda F, Codazzi M, Salerni B (2012) Primary extra-gastrointestinal stromal tumor of retroperitoneum. Clin Med Insights 6:189–197
11. Takao H, Yamahira K, Doi I, Watanabe T (2004) Gastrointestinal stromal tumor of the retroperitoneum: CT and MR findings. Eur Radiol 14:1926–1929
12. Özkavukcu E, Aygün S, Erden A, Savaş B (2009) Pelvic retroperitoneal angioleiomyoma mimicking a uterine mass. Diagn Interv Radiol 15:262–265
13. Rha SE, Byun JY, Jung SE, et al. (2003) Neurogenic tumors in the abdomen: tumor types and imaging characteristics. RadioGraphics 23(1):29–43
14. Lonergan GJ, Schwab CM, Suarez ES, Carlson CL (2002) Neuroblastoma, ganglioneuroblastoma, and ganglioneuroma: radiologic–pathologic correlation. RadioGraphics 22:911–934
15. Brennan C, Kajal D, Khalili K, Ghai S (2014) Solid malignant retroperitoneal masses—a pictorial review. Insights Imaging 5:53–65
16. Goh BK, Tan YM, Chung YF, et al. (2006) Retroperitoneal schwannoma. Am J Surg 192:14–18
17. Kalra N, Vijayanadh O, Lal A, et al. (2005) Retroperitoneal plexiform neurofibroma mimicking psoas abscesses. Australas Radiol 49:330–332
18. Bass JC, Korobkin M, Francis IR, Ellis JH, Cohan RH (1994) Retroperitoneal plexiform neurofibromas: CT findings. Am J Roentgenol 163:617–620
19. Wasa J, Nishida Y, Tsukushi S, et al. (2010) MRI features in the differentiation of malignant peripheral nerve sheath tumors and neurofibromas. Am J Roentgenol 194:1568–1574
20. Ueno T, Tanaka YO, Nagata M, et al. (2004) Spectrum of germ cell tumors: from head to toe. RadioGraphics 24:387–404
21. Soydinc HE, Sak ME, Evsen MS, Bozkurt Y, Keles A (2012) Unusual case of extraovarian granulosa cell tumor. Eur Rev Med Pharmacol Sci 16(4):30–31
22. Caiafa RO, Vinuesa AS, Izquierdo RS, et al. (2013) Retroperitoneal fibrosis: role of imaging in diagnosis and follow-up. Radiographics 33:535–552